*Proceedings of the 16th International Conference on Soil Mechanics and Geotechnical Engineering*

*doi:10.3233/978-1-61499-656-9-1443*

# Observed bracing responses at the Ford Design Center excavation

## Comportement des ètais sur l'excavation du Ford Design Center

J. Tanner Blackburn, Kate Sylvester & Richard J. Finno*
*Department of Civil and Environmental Engineering, Northwestern University, USA*
*r-finno@northwestern.edu*

ABSTRACT

The relative contributions of temperature, earth pressurs and construction loading on the resulting stresses in excavation support members were evaluated by analyses of the results of strain gauge measurements obtained at a 10 m deep excavation through clay. Temperature impacted both axial and bending stresses in the supports. It is shown that axial thermal loading may constitute 50% of the axial strut load. Bending stresses developed as a result of thermal variations through the cross-section of a support member, self-weight of the supports, and unexpected construction loadings. The bending introduced large stresses as well. The proximity of a support member to a corner of the excavation had little effect on the stress in the member.

RÉSUMÉ

Les effets relatifs de la température et du poids du sol sur les contraintes dans les étais ont été comparés après analyse des resultats provenant de mesures de tension de jauge pour une excavation de 10 m de profondeur à travers de l'argile. La température influencait a la fois les contraintes axiales et de flexion dans les supports. Il est montré que l'influence de la température peut representer jusqu'a 50% de la composante axiale du poids. Les contraintes de flexion résultent des variations thermiques à travers les sections des etais, le poids propre des etais et les charges imprévisibles duent au chantier en construction. La flexion produit également des contraintes importantes. Le fait qu'un support soit pres d'un coin de l'éxcavation n'a presque pas d'effet sur la contrainte dans ce support.

## 1 INTRODUCTION

As part of the monitoring program for the excavation for the Ford Engineering Design Center on the Evanston campus of Northwestern University, strain gauges were placed at the midpoints of cross-lot bracing and diagonal support members. The excavation was 10 m deep and included a sheet-pile wall supported by two levels of internal braces. This paper summarizes the conditions at the site and presents the results of the analyses of the strain gauge data. An analysis of the strains in the bracing elements due to earth pressure, temperature and bending was conducted. The relative contributions of each are presented.

## 2 PROJECT DESCRIPTION

A plan view of the support system at the site is shown in Figure 1. The soil stratigraphy consists of 5 m of sandy urban fill overlaying a 1 meter clay crust, 4.3 m of soft clay and 7.9 m of medium clay. Two levels of lateral bracing were used to support the sheet pile walls. The top (T) and bottom (B) level bracing elements are listed in Table 1. All support elements had a nominal yield stress of 250 MPa. The loads from the retained soil were transferred to the struts via wide-flange beam walers. Vertical plates were welded to the sheeting and the walers so that the sheeting was in contact with the walers before the struts were installed. The struts were set in place, subjected to an axial load, and welded to the walers.

Data were collected using vibrating wire strain gauge pairs, installed on opposite sides of the support members, as shown on Figure 2. Strain gauge pairs were employed to separate bending and axial stresses. The axial strut load, at the neutral axis, was calculated from the average of the four strain gauge readings, when all four gauges were operational. Two gauges were placed in the center of the web of the wide flange sections. The strain gauge pairs also provided an opportunity to observe bending stress development during construction, which was attributable to several factors, as subsequently discussed.

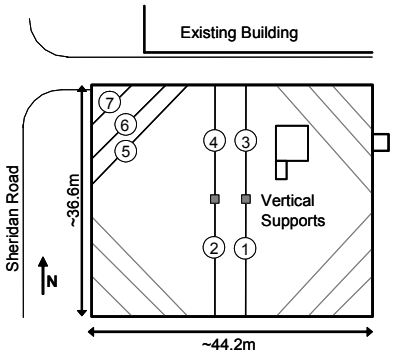

Figure 1: Plan View of Site

Table 1: Support element labels and descriptions

| Element | Label | Structural Properties |
|---|---|---|
| Strut | T-1 to T-5 | 0.61m (24") O.D., 1.27cm (0.5") Thickness |
| | T-6 | 0.46m(18") O.D., 1.27cm (0.5") Thickness |
| | T-7 | W14x145 |
| | B-3/4/6 | 0.61m (24") O.D., 1.27cm (0.5") Thickness |
| | B-5 | 0.66m (26") O.D., 1.27cm (0.5") Thickness |
| | B-7 | W14x193 |
| Waler | Top | W24x141 |
| | Bottom | W36x230 |

The thermal properties of the gauges were closely matched to those of the steel struts and the slight difference in coefficients of thermal expansion was accounted for during data reduction. The original gauge datum corresponds to the value recorded when the strut was first placed atop the wales, prior to permanent welding to the wall. The observed strain includes contributions from earth pressure, axial thermal loading, thermal bending, and construction-induced bending. The data does not include bending stresses that arise for the self-weight of the member.

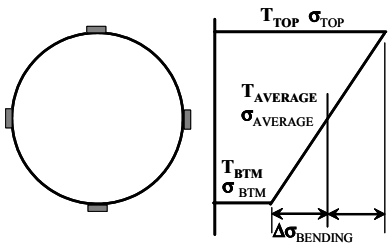


Figure 2: Support member cross section with strain gauges and stress and temperature values

## 3 AXIAL LOADS

### 3.1 *Thermal Expansion and Contraction*

Because the support members are neither free to expand and contract, nor fixed, the approach described by Boone and Crawford (2000) was used to generate an approximation of the degree of fixity of the support members, and thus to calculate the thermally-induced axial stress. Because the Ford Center support members were welded to the walers rather than shimmed in place as they were in the excavation Boone studied, Boone's model was adjusted to account for resistance to contraction. The reset temperature in Boone's model, which prevents calculation of any negative or contractive stress was replaced with the initial reference temperature. When the temperature drops below this reference temperature there is a separate factor to account for the resistance to contraction. Thus the empirical calculation of the change in axial load due to temperature is determined by:

$$\Delta P_i = m\Delta T_i, \quad (1)$$

where $\Delta P_i$ is the incremental difference in strut load (between two consecutive readings), $\Delta T_i$ is the incremental difference in temperature, and $m$ is a thermal stiffness coefficient, either $m_{exp}$ or $m_{ctr}$, depending on whether the strut expands or contracts.

Two thermal load coefficients are required when Boone's model is modified in this way because the degree of fixity of each strut as it relaxes due to a decrease in temperature tension ($m_{ctr}$) is different from its degree of fixity as it expands due to an increase in temperature ($m_{exp}$). To eliminate the effects of a rather erratic excavation pattern, only temperature and load change data measured after the excavation reached final grade were used to calculate the thermal expansion and contraction coefficients. Data were collected over a period of 2.5 months with a strut temperature range of 14 to 48 ºC. Typical results, for strut T-6, are shown on Figure 3. A comparison of the empirical and theoretical $m$ coefficients presented in Table 2.

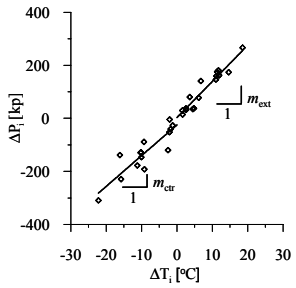


Figure 3: Typical incremental axial force versus incremental temperature obtained after the final excavation depth was attained

Table 2. Empirical and theoretical thermal load coefficients

| Strut | αEA (strut) | $m_{expansion}$ (kN/ºC) | $m_{contraction}$ (kN/ºC) | $m_{tg}$ *(MPa//*ºC) | |
|---|---|---|---|---|---|
| | | | | Vert. | Hor. |
| T-1 | 55.7 | 14.2 | 12.7 | 1.48 | |
| T-2 | 55.7 | gauges destroyed | | | |
| T-3 | 55.7 | 15.5 | 14.7 | 1.02 | |
| T-4 | 55.7 | 11.2 | 10.3 | 1.16 | 1.42 |
| T-5 | 55.7 | 12.1 | 8.5 | 1.29 | |
| T-6 | 41.5 | 13.6 | 11.6 | 0.50 | |
| T-7 | 63.2 | 18.6 | 14.8 | W14x145 | |
| B-3 | 55.7 | 22.5 | 17.6 | 1.66 | |
| B-4 | 55.7 | 12.9 | 15.2 | 1.57 | 2.09 |
| B-5 | 60.5 | 15.8 | 13.3 | 1.63 | |
| B-6 | 55.7 | 20.6 | 19.2 | 0.52 | |
| B-7 | 86.6 | 20.4 | 19.8 | W14x193 | |

The $m$ data on columns 3 and 4 in Table 2 show that the thermal load coefficients were generally larger for the lower support level, as a result of the greater resistance provided by the soil at depth and the larger walers used in the lower level. All coefficients were approximately 25% of the theoretical value based on conditions of full fixity. The $m$ coefficients for strut relaxation as a result of decreasing temperature were slightly smaller than those for strut expansion, but clearly greater than 0, as assumed in the Boone procedure. This observation emphasizes the need to account for structural details of the retention system when evaluating temperature-induced axial loads.

### 3.2 *Earth Pressure*

By employing the thermal axial load coefficients, the observed strut load can now be separated into thermal and earth components by:

$$P_{EARTH} = P_{OBSERVED} - m\Delta T, \quad (2)$$

where $P_{OBSERVED}$ is the axial force at the neutral axis, $\Delta T$ is the change in temperature since strut installation, and $m$ is either $m_{ext}$ or $m_{ctr}$.

Figure 4 shows measured axial loads and the calculated earth pressure loads in each support member as well as the loads imputed based on the Terzaghi and Peck apparent earth pressure envelope (Peck, 1969). Also shown is a summary of the construction record for the excavation. The Terzaghi and Peck calculation is an empirical estimation of the maximum load a member will experience, and is marked by a dashed line in Figure 4. The line marked by open circles indicates measured loads, while the data line marked by solid circles indicates thermally-corrected earth pressure loads.

The loads in the supports were negligible a short time after preloading, indicating the there was sufficient relaxation of the newly-welded connections to render the preload force equal to zero prior to excavation below the support. The loads in the upper support level increased as the excavation depth increased, but stabilized or decreased following the lower level support installation. The loads in the lower supports gradually increased after installation until the bottom of the excavation was reached, and were relatively constant until the lower level braces were removed. These observations indicate the load transfer to the lower level supports increased as the excavation deepened.

Also clear in Figure 4 are the responses during removal of the bottom level supports, wherein the loads in the top struts increase considerably. This increase in load due to detensioning of the bottom supports must be accounted for during support system design.

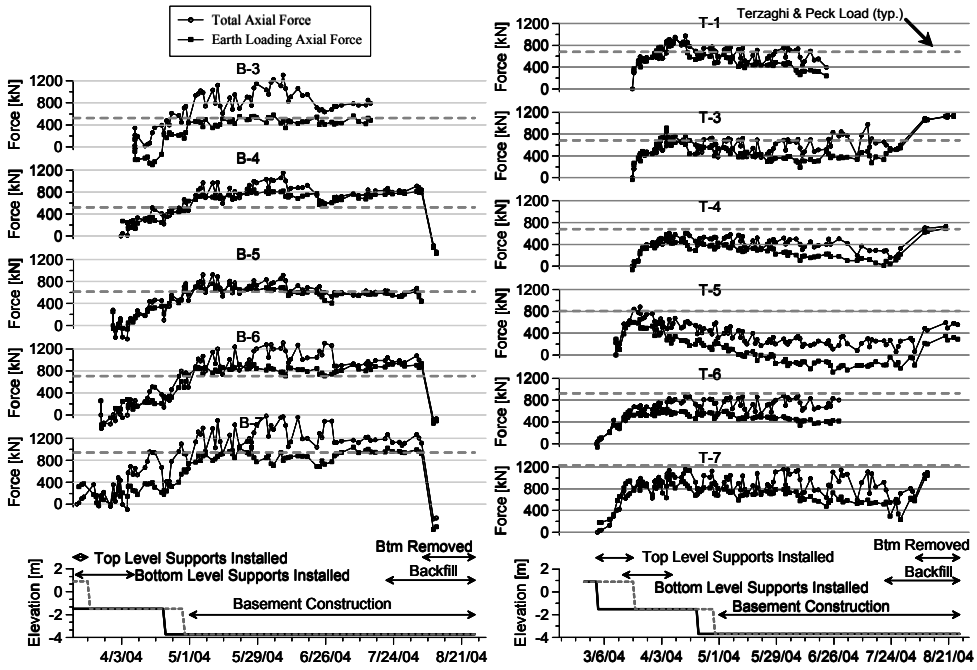


Figure 4: Axial loads in struts

The measured axial loads exceeded the Terzaghi and Peck estimate for the lower support members, whereas the upper level supports carried maximum loads consistent with the Terzaghi and Peck estimates.

## 4 BENDING STRESSES

The axial loads calculated in Section 3 indicate the state of stress along the neutral axis of the support members. However, the highest stresses in the support members were a result of the combined effects of axial load and bending caused by thermal stress gradients, self-weight and unanticipated construction loadings.

### 4.1 *Thermal Stress Gradients*

Thermal stress gradients across support member cross-sections caused significant bending stresses at this site because the bracing was subjected to direct sunlight. As is the case with axial loads, a simple calculation of the bending stress would not be accurate because of the intermediate degree of fixity of the support members. Consequently, an empirical relationship was developed between changes in extreme fiber stress, $\Delta\sigma$, and the temperature difference in opposite gauges via a temperature gradient coefficient, $m_{tg}$. A

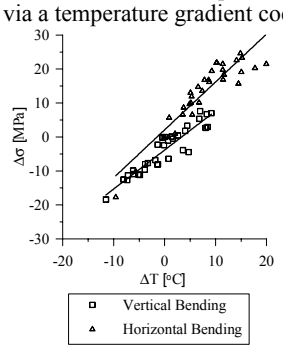


Figure 5: Typical relation between stress and temperature changes on opposite sides of a strut

Note that $\Delta\sigma$ is twice the bending stress. A typical relation between extreme fiber stress and temperature is shown on Figure 5, and the values of $m_{tg}$ for all gauge pairs with sufficient available data are shown in Table 2.

Similar to the thermal load coefficients, the values of $m_{tg}$ for the bottom struts in the vertical direction generally are higher than those for the top struts. The values of $m_{tg}$ in the horizontal direction are about 25% higher than those in the vertical direction, suggesting slightly more rotational restraint in the horizontal than vertical directions.

### 4.2 *Self-weight Bending*

Bending stress due to member self-weight was not measured by the strain gauges. The gauges were installed after the support members were dropped into place, prior to permanent attachment to the wall and waler; thus bending due to self-weight had already occurred when the initial reference strain was recorded. However, approximating the structure as a uniformly loaded pipe strut or H-pile, the bending stress at the extreme fibers was calculated to be as much as 25 MPa, assuming partial restraint at the ends of the beams with the moment at the strain gage locations at the mid-point of a strut computed as $1/16\ wl^2$.

### 4.3 *Construction-induced Bending*

Bending stresses developed in several of the cross lot braces due to construction of a ramp during excavation, as shown in Figure 6. The stresses observed at the top and bottom fibers during this period are shown in Figure 7. While this ramp was in place, the bending stress reached 125 MPa or about ½ the yield stress. These bending stresses can be calculated with sufficient accuracy by assuming the soil applied a linearly decreasing load over the portion of a beam that was covered, with the maximum pressure corresponding to the height of soil at the wall and assuming the strut was pinned at the wall and the intermediate lateral brace.

Figure 6: Photograph of temporary access ramp on cross-lot struts.

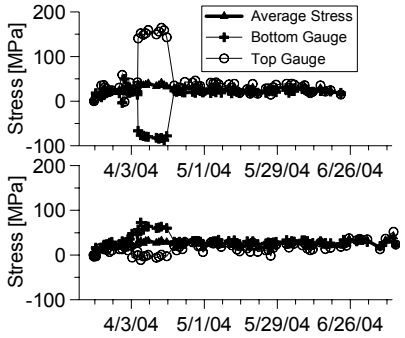


Figure 7: Difference in stress levels observed by top and bottom gauges of southeast (top) and northeast (bottom) struts.

## 5 SUMMARY OF STRESSES

A summary of the maximum extreme fiber stresses in each strut is given in Figure 8. The data show that the most severe loading condition arose from the unanticipated (in design) ramp construction. Without that loading, fairly consistent trends were observed. The stresses caused by axial loads were about equal to those caused by bending. Temperature induced axial loads and bending stresses were significant and were responsible for about one-half of each component. With the exception of the ramp loading, all other causes resulted in stress levels of about 80 MPa, well below the yield stress of 250 MPa. The contractor used in-stock structural elements as the bracing, and did not attempt to optimize their size. This was fortunate given the unanticipated loading on several of the cross-lot braces by the excavator's temporary ramp.

## 6 CORNER EFFECTS

Figure 9 shows the calculated tributary earth pressure versus distance from the excavation corner to observe any corner loading effects. Little or no increase in stress with distance from the corner of the excavation was observed. The 3-d effects apparently did not extend appreciable distance from the corners, in accordance with guidelines suggested by Finno and Roboski (2005) for evaluating the extent of 3-d effects for a given excavation geometry and flexible wall system.

## 7 CONCLUSIONS

Earth loads, temperature effects and construction loads significantly affected the stresses in the struts at the excavation for the Ford Center. Thermal and self-weight bending induced stresses approximately equal to those arising from earth pressure and thermally-induced axial loads. Construction of a temporary ramp that was not anticipated in design induced higher stresses than all other causes. Corner effects were relatively insignificant at this site.

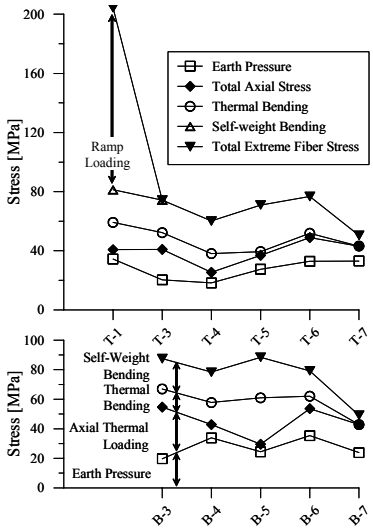


Figure 8: Summary of stresses in struts

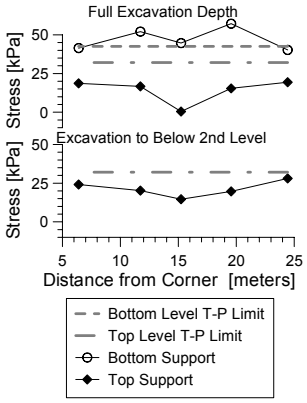


Figure 9: Variation of tributary earth pressure with distance from corner

## ACKNOWLEDGEMENTS

This work was supported in part by grant CMS-0219123 from the National Science Foundation (NSF) and a grant from the Infrastructure Technology Institute at Northwestern University. The second author was funded by a Research Experience for Undergraduates grant from NSF. The interest and cooperation of Mr. Michael Wysockey of Thatcher Engineering Corp., the excavation support subcontractor, and Mr. Phil Blakeman of Turner Construction Co., the general contractor, is greatly appreciated.

## REFERENCES

Boone, S.J. and Crawford, A.M. (2000). "Braced Excavations: Temperature, Elastic Modulus, and Strut Loads." *J. Geotech. Geoenviron. Eng.,* 126(10), 870-881

Finno, R. J., and Roboski, J. F. (2005). "Three-Dimensional Response of a Tied-Back Excavation through Clay." *J. Geotech. Geoenviron. Eng.,* 131(3), March, 2005

Peck, R.B. (1969). "Deep excavations and tunneling in soft ground: State-of-the-art report." *Proc. 7th Int. Conf. on Soil Mech. And Found. Engrg., Sociedad Mexicana de Mecanica de Suelos*, Mexico City, 225-290.